Int. J. Heat Mass Transfer. Vol. 22, pp. 447–459

0017-9310/79/0301-0447 $02.00/0

PREDICTION AND MEASUREMENT OF THE THERMAL CONDUCTANCE OF LAMINATED STACKS

T. N. VEZIROĞLU,* A. WILLIAMS,*† S. KAKAÇ‡ and P. NAYAK*

(*Received* 28 *April* 1978)

Abstract—This paper presents a novel theoretical analysis of the thermal contact conductance between thin metallic sheets. Previous theories apply only to conditions where the metal thickness is large compared with the diameter of the typical contact zone. The new theory developed herein is used to predict the conductances of stacks of laminations over a wide range of contact pressure and with various interstitial fluids. Metallic discs of stainless steel, brass and transformer core steel were tested, and measured conductances were compared with predictions. The agreement between theory and experiment was good, both for the tests conducted in this program and for the available published experimental data.

NOMENCLATURE

- a, half width of contact element for planar contacts or radius of contact element for circular contacts;
- b, radius of actual contact spot;
- B, non-dimensional thickness parameter $(= d/a)$;
- C, non-dimensional constriction parameter $(= b/a)$;
- d, fluid thickness;
- D, non-dimensional length parameter $(= l/a)$;
- G, coefficients of terms in equation (12);
- K, thermal conductivity;
- l, axial length of contact element;
- ξ, dimensionless constant of equation (11);
- m, n, number of terms considered in equation (17);
- p, exponent of integrating factor in equation (16);
- Q, heat flux;
- R, resistance;
- T, temperature;
- u, conductance;
- U, non-dimensional contact conductance;
- x, y, z, coordinates;
- λ, positive roots of equation (13);
- ϕ, function of $\left(\lambda \frac{x}{a}\right)$ in equations (14) and (15).

Subscripts

- 0, total with no constriction;
- 1,2, refer to parameters on sides 1 and 2 of contact element;
- f, fluid;
- s, solid harmonic mean;
- T, total;
- c, constriction.

*University of Miami, Coral Gables, Florida, U.S.A.
†Visiting professor.
‡Middle East Technical University, Ankara, Turkey.

1. INTRODUCTION

LAMINATED materials are in common use in engineering. Electrical transformers, motors and generators contain components made of thin sheets of metal (usually iron or steel) clamped together, with an insulating film of enamel or varnish between adjacent sheets. These components suffer magnetic or electrical losses which result in undesirable heat generation, which might cause overheating, with consequent damage to the machine. The removal of heat from such components is made difficult in the direction normal to the plane of laminations, as each pair of adjacent laminations offers a contact resistance in the heat flow path. The effective thermal conductivity normal to the laminations may be as low as 5% of the conductivity along the plane of the laminations.

The contact resistance arises as a result of the imperfect contacts between adjacent faces. The main parameters affecting the resistance are the clamping pressure, the hardness of the materials, the shapes of the surface roughnesses, the thermal properties of the metals in contact and the interstitial fluid, etc. By the appropriate selection of these parameters one can design a stack of laminations with a very high resistance, making it suitable for the support for cryogenic vessels. On the other hand, in electrical machines the parameters are adjusted to give a low thermal resistance thereby relieving the problem of heat dissipation.

The purpose of this paper is to examine the influences of some of the above mentioned parameters of stacks of laminations, and to compare experimental results with predicted values for a variety of conditions.

2. LITERATURE SURVEY

The subject of heat flow across metallic contacts has received much attention in recent years, and most of its problems are now understood and documented. One aspect which has remained relatively unexplored is that of heat flow through laminated materials, and this brief survey is re-

stricted to publications relevant to this configuration. The main difference between the conditions of heat flow through the contact between bulky components and those pertaining to thin laminations is in the shapes of the heat flow lines or isotherms in the contacting components. The restricted heat flow paths of the laminated components greatly complicate the theoretical analysis of contact conductance. Almost all of the reported work is on experimental, rather than on theoretical, determinations of contact conductance.

The pressure of a thermal resistance is beneficial if the component is required to be an insulator. Mikesell and Scott [1] made use of this resistance to construct an insulating support member for a cryogenic tank. Their member consisted of a stack of thin, bare, metallic sheets, held together by the weight of the tank and its contents. The effective conductivity of this member was as low as 2% of the conductivity of the material forming the member. They found that the insulation value varied directly with the number of contact elements. They did not present a theoretical analysis of their results.

Thomas and Probert [2] measured the conductances of multi-layer contacts comprising steel, brass, mylar, dacron and titanium alloy components. The tests were performed at low temperatures, to obtain data for the design of insulating supports for cryogenic equipment. They were able to make recommendations to assist with designs of this type.

Whereas, the previous references were directed towards minimizing the thermal conductance, the requirements of laminated components in electrical equipment are for high conductance values. Transformer cores, electric generator and motor armatures, and stators, all suffer losses which appear as a heat load on the machine. The design of the machine is influenced by the thermal requirements, and this influence increases with the size of the equipment. For instance, the stator core of a large turbogenerator may be required to dissipate several megawatts of heat from a very restricted volume. The cooling system is a major consideration in the design of this component.

Roberts [3] examined the thermal problems of electrical machinery and conducted tests to measure the thermal diffusivities of several types of electrically insulated laminations as used in the stator cores of large turbogenerators. He derived the conductivities from the measured diffusivities. Tests were performed in an environment of air at normal atmospheric pressure; which is usual for the stator core of a large turbogenerator containing hydrogen at several atmospheres pressure. In view of the fact that the thermal conductivity of the interstitial fluid is an important factor in determining the contact conductance, Roberts' experimental results are not directly applicable to the analysis of heat flow in generators.

Williams [4] proposed a theoretical model to predict the thermal contact conductance of enameled sheets and applied this to Roberts' test results to predict the thermal conductivities in various environments. The model relies on the separation of the contributions to contact conductance due to the solid contacts and to the interface fluid. He predicted that typical generator cores would have thermal conductivities (across the laminations) about seven times higher when immersed in hydrogen than when immersed in normal atmospheric air.

Support for the model was given by test data of Williams [5] on a variety of materials in environments of air, vacuum, and helium. The latter was used instead of hydrogen for safety reasons. The clamping pressure was varied over a range of 50–150 lbs/in^2 to represent conditions typical of service in turbogenerators. The surface finishes of the enameled plates covered a range of CLA from 4 μin to 55 μin. It was found by measurement that in normal atmospheric environments, the smoothness of the lamination played a prominent part in the contact conductance (which itself was the main factor in overall conductance). However, as the conductivity of the interface fluid was increased, the thermal load was carried mainly by the interface fluid rather than by the solid contacts, so that with hydrogen as the environmental fluid, the proportion of heat load carried by the solid contacts became almost negligible. A single value of conductivity was proposed for all the types of laminations tested and for all contact pressures within the range of the test. This possibly surprising conclusion has not been challenged, nor has it been confirmed by published data. Manufacturers of large electrical turbogenerators must perform full-scale testing of their machinery to determine satisfactory overall operation and are naturally reluctant to publish data of their detailed findings. Even so, it is unlikely that testing of full-scale machines would be instrumented sufficiently to establish fundamental properties such as thermal conductivities, as it is commercially impractical to undertake sufficiently-detailed measurements.

There have been several investigations of heat flow across plated contacts. The effect of plating a hard, roughly-surfaced metal with a soft covering of highly conductive metal; e.g. gold, indium, etc., may be highly beneficial in improving the contact conductance of a joint. Mikic and Carnasciali [6] developed a theoretical model of the contact which gave good agreement with their experiments on specimens of stainless steel with copper-plated surfaces. They point out that both elements of a contact should be similarly plated to achieve the highest conductance values.

The introduction of soft, highly-conducting foils between contacts of hard metals has also been shown to improve contact conductance. Molgaard and Smeltzer [7] measured the thermal behavior of gold foils between iron and copper, also iron and platinum/rhodium elements over wide ranges of pressure and temperature. Fletcher [8, 9] has exam-

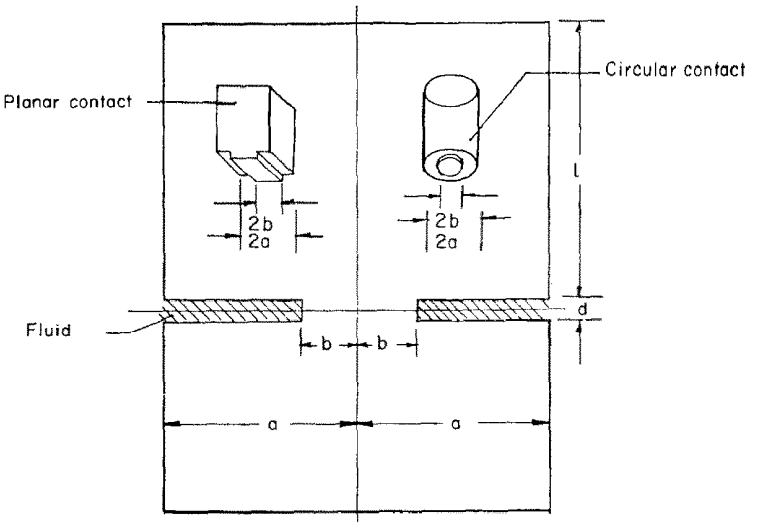

FIG. 1. Cross-section of typical microscopic contact element.

ined the effects of various gasket materials intended for use in the joints of space crafts.

Almost all of those investigations have been directed towards obtaining improvements in contact conductance. Unavoidable features, such as the presence of surface films, which inhibit conductance, are usually regarded as undesirable, especially for conditions of high heat flux; e.g. from the fuel to its sheath in a nuclear reactor. Such films are, fortunately, less influential on the thermal contact conductance than they are on the electrical contact conductance, but, nevertheless, cannot be ignored. Gale [11] and Tsao and Heimburg [12] examined surface films (mostly oxides) on aluminum contacts of both smooth and rough types and concluded that smooth contacts can be substantially affected by their films.

The extreme thinness of absorbed or contaminant films makes their effects dissimilar from "thick" films, such as enamel coatings. The material properties of thin films usually cannot be specified with confidence. For instance, their thermal conductivities are not those of the bulk material because of the conducting "tunnel effect"; also, their strengths are greatly affected by those of the underlying metals. Thin films may not be consistent in their effects as they may crack or rupture during the course of loading a contact. Although thin, electrically-insulating films may be attractive to the designers of certain types of electrical equipment, their unpredictability usually precludes their use. Instead, the designer must incorporate a thicker, more reliable form of electrical insulation which, unfortunately, may introduce problems by nature of its thermal insulation. Coated surfaces are, therefore, in common usage. The fact that the coating is intimately bonded with the underlying material makes the contact characteristics different from those of gaskets or foils. The coating may not distort freely, as may a gasket. The presence of trapped air or fluid in a gasketed joint is, obviously, inapplicable at the coated surface.

A theoretical analysis of the influence of interstitial plates on thermal conductance was presented by Veziroğlu *et al.* [10] who compared their predictions with experimental results of seven different interstitial materials. The agreement was good for all of the metallic interstitial plates, but poor for mica. The latter was attributed to the irregular behavior of thin sheets of mica.

3. THEORY

3.1. *Formulation of problem*

When two surfaces are pressed together, the usual model of the contact configuration is of a series of microscopic real contact spots connected to cylindrical elements of the base material. Usually the radius of the average contact spot is very small compared with the length of the region feeding it, and it is often acceptable to treat the latter as a semi-infinite half space. However, for thin sheets in contact it is necessary to account for the finite thickness of the region feeding heat through the actual contact spot.

Figure 1 shows a contact element cross-section which applies to both planar and circular contacts. Translation of the cross-section normal to x–y plane would generate a planar contact element, and rotation around y-axis would generate a circular contact element. One quarter element is shown in Fig. 2. The dimension "a" is the contact element half width for planar contacts and the contact radius for circular contacts, and "b" is the actual contact radius for circular contacts. The fluid layer thickness, which is small compared to the contact element dimensions, is "d". The x-axis is located such that it divides the fluid layer thickness in the ratio K_2/K_1, i.e.

$$d_1 = d \cdot K_2/(K_1 + K_2) \tag{1}$$

and

$$d_2 = d \cdot K_1/(K_1 + K_2), \tag{2}$$

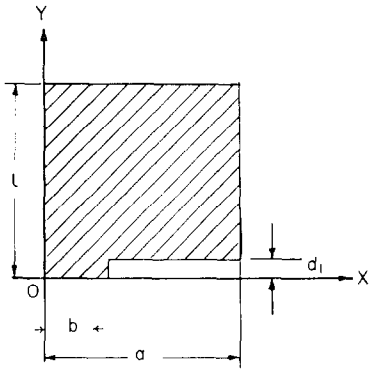

FIG. 2. Quarter element used for evaluation of temperature field.

where d_1 and d_2 are the fluid layer thickness between the x-axis and solids 1 and 2, respectively. Then the system becomes symmetrical from the heat transfer point of view with respect to a plane passing through x-axis and normal to y-axis. Therefore, only the $X0Y$ quarter plane is considered. The steady state temperature distribution in solid 1 satisfied Laplace's equation,

$$\frac{\partial^2 T}{\partial x^2}+\frac{P}{x}\cdot\frac{\partial T}{\partial x}+\frac{\partial^2 T}{\partial y^2}=0, \tag{3}$$

where $P=0$ for planar contacts, and $P=1$ for circular contacts. The assumed boundary conditions of the problem are:

$$\frac{\partial T(0,y)}{\partial x}=0 \qquad 0<y<L \tag{4}$$

$$\frac{\partial T(a,y)}{\partial x}=0 \qquad 0<y<L \tag{5}$$

$$T(x,l)=T_1 \qquad 0<x<a \tag{6}$$

$$T(x,0)=0 \qquad 0<x<b \tag{7}$$

$$K_1\frac{\partial T(x,0)}{\partial y}=\frac{K_f T(x,0)}{d_1} \qquad b<x<a, \tag{8}$$

where K_1 and K_f are thermal conductivities of solid 1 and the interstitial fluid respectively. Let K_s be the harmonic mean of the thermal conductivities of solid 1 and 2, then boundary condition (8) can be written as follows:

$$\frac{\partial T(x,0)}{\partial y}=\frac{2KT(x,0)}{d}, \tag{9}$$

where

$$K=\frac{K_f}{K_s}, \quad \text{and} \quad K_s=\frac{2K_1K_2}{K_1+K_2}. \tag{10}$$

To ensure that the results will also be valid for $K_f=0$ (i.e. the contact in vacuum) the LHS of equation (9) can be made the same as that of equation (7) by adding $\xi T/a$ to both sides of equation (9). The dimensionless constant ξ acts as the damping factor in obtaining convergence. After performing the above operation and combining equation (7), one can write

$$T(x,0)=\begin{cases}0 & 0<x<b\\ \dfrac{a}{\xi}\dfrac{\partial T(x,0)}{\partial y}+\left[1-\dfrac{2K}{\xi\cdot B}\right]T(x,0) & b<x<a\end{cases} \tag{11}$$

where

$$B=\frac{d}{a}.$$

3.2. *Solution*

The solution to equation (3) with boundary conditions (4)–(6) and (11) is given by

$$T(x,y)=T_1+\frac{\xi-y}{a}G_0-\sum_{n=1}^{\infty}\frac{G_n}{\lambda_n}\phi\left(\lambda_n\frac{x}{a}\right)\sinh\frac{\lambda_n(\xi-y)}{a} \tag{12}$$

where G's are constants to be determined and λ's are the positive roots of equation

$$\frac{\partial\phi\left(\lambda_n\dfrac{x}{a}\right)}{\partial x}=0 \quad \text{at} \quad x=a, \tag{13}$$

where function ϕ is

$$\phi\left(\lambda_n\frac{x}{a}\right)=\cos\left(\lambda_n\frac{x}{a}\right) \tag{14}$$

for a planar contact, and

$$\phi\left(\lambda_n\frac{x}{a}\right)=J_0\left(\lambda_n\frac{x}{a}\right) \tag{15}$$

for a circular contact. A negative sign has been introduced in equation (12) to make all G_n's positive.

The zeroth coefficient G_0 can be obtained by substituting equation (12) in equation (11) and multiplying both sides by $x^p\,dx$ and integrating over the region $x = 0$ to $x = b$. With proper dimensionless parameters, one obtains

$$G_0 = \frac{p+1}{DC^{p+1}} \sum_{n=1}^{\infty} \frac{G_n}{\lambda_n} \sin(\lambda_n D) \int_0^C \phi(\lambda_n x) x^p \, dx - \frac{1}{D}. \tag{16}$$

Substituting equation (12) in equation (11) and multiplying both sides by $x^p\phi(\lambda_m x)$ and integrating over the region $x = C$ to $x = 1$ one obtains

$$\begin{aligned} -\frac{1}{D}\int_0^C x^p\phi(\lambda_m x)\,dx = {} & -\frac{\xi G_m}{\lambda_m}\sinh(\lambda_m D)\int_0^1 x^p\phi^2(\lambda_m x)\,dx \\ & - \sum_{n=1}^{\infty} G_n\left[\cosh(\lambda_n D) - \left(\xi - \frac{2K}{B}\right)\frac{\sinh(\lambda_n D)}{\lambda_n}\right]\int_C^1 x^p\phi(\lambda_n x)\phi(\lambda_m x)\,dx \\ & + \left(\xi - \frac{2K}{B} - \frac{1}{D}\right)\frac{p+1}{C^{p+1}}\sum_{n=1}^{\infty}\frac{G_n}{\lambda_n}\sinh(\lambda_n D)\int_0^C x^p\phi(\lambda_m x)\,dx, \end{aligned} \tag{17}$$

where $m = 1, 2, 3, \ldots, \infty$ and $n = 1, 2, 3, \ldots, \infty$.

Equations (17) form a set of linear equations in terms of unknown G_n's and G_m's. They can be evaluated by considering a large number (N) of unknowns and an equal number of equations (17). After G_1 through G_n's are calculated, the zeroth coefficient G_0 can be obtained from equation (16). For a planar contact equation (17) reduces to

$$\begin{aligned} -\frac{2\sin(m\pi C)}{m\pi D} = {} & G_m\left\{-\frac{L}{m\pi}\sinh(m\pi D) - \left[\cosh(m\pi D) - \left(\xi - \frac{2K}{B}\right)\frac{\sinh(m\pi D)}{m\pi}\right]\right. \\ & \times\left[1 - C - \frac{\sinh(2\pi mC)}{2\pi m}\right] + \left(\xi - \frac{2K}{B} - \frac{1}{D}\right)\left.\frac{\sinh(m\pi D)2\sin^2(m\pi C)}{m^3\pi^3 C}\right\} \\ & + \sum_{\substack{n=1 \\ n\neq m}}^{\infty} G_n\left[\cosh(n\pi D) - \left(\xi - \frac{2K}{B}\right)\frac{\sinh(n\pi D)}{n\pi}\right]\left[\frac{\sin(n-m)\pi C}{(n-m)\pi} + \frac{\sin(n+m)\pi C}{(n+m)\pi}\right] \\ & + \left(\xi - \frac{2K}{B} - \frac{1}{D}\right)\sum_{n=1}^{\infty} G_n \sinh(n\pi D)\frac{2\sin(n\pi C)\sin(m\pi C)}{n^2 m\pi^3 C}, \end{aligned} \tag{18}$$

where $m = 1, 2, 3, \ldots, \infty$.

For a circular contact, equation (17) reduces to

$$\begin{aligned} \frac{2CJ_1(\lambda_m C)}{\lambda_m D} = {} & G_m\left\{\xi\frac{\sinh(\lambda_m D)}{\lambda_m}J_0^2(\lambda_m) + \left[\cosh(\lambda_m D) - \left(\xi - \frac{2K}{B}\right)\frac{\sinh(\lambda_m D)}{\lambda_m}\right]\right. \\ & \times\left[J_0^2(\lambda_m) - C^2J_0^2(\lambda_m C) - C^2J_1^2(\lambda_m C)\right] - \left.\left(\xi - \frac{2K}{B} - \frac{1}{D}\right)\frac{4}{\lambda_m^3}\sinh(\lambda_m D)J_1^2(\lambda_m C)\right\} \\ & - \sum_{\substack{n=1 \\ n\neq m}}^{\infty} G_n\left[\cosh(\lambda_n D) - \left(\xi - \frac{2K}{B}\right)\frac{\sinh(\lambda_m D)}{\lambda_n}\right]\frac{2c}{\lambda_n^2 - \lambda_m^2}\left[\lambda_n J_0(\lambda_m C)J_1(\lambda_n C)\right. \\ & \left. - \lambda_m J_0(\lambda_n C)J_1(\lambda_m C)\right] - \left(\xi - \frac{2K}{B} - \frac{1}{D}\right)\sum_{\substack{n=1 \\ n\neq m}}^{\infty} 4G_n\sinh(\lambda_n D)\frac{J_1(\lambda_n C)J_1(\lambda_m C)}{\lambda_n^2\lambda_m}, \end{aligned} \tag{19}$$

where $m = 1, 2, 3, \ldots, \infty$.

Figures 3 and 4 show the theoretical constriction number (C) plotted against u for planar and circular contacts when k is zero.

3.3. *Heat transfer*

The heat flux through specimen can be calculated as follows:

$$= -Q = \int_0^a (2\pi x)^p\,dx\,K_1\left(\frac{\partial T}{\partial y}\right)_{y=l} \tag{20}$$

$$= -(2\pi)^p K_1 \frac{G_0 a^p}{(p+1)} + (2\pi)^p K_1 \sum_{n=1}^{\infty}\frac{G_n}{a}\int_0^a x^p\phi\left(\lambda_n\frac{x}{a}\right)dx. \tag{21}$$

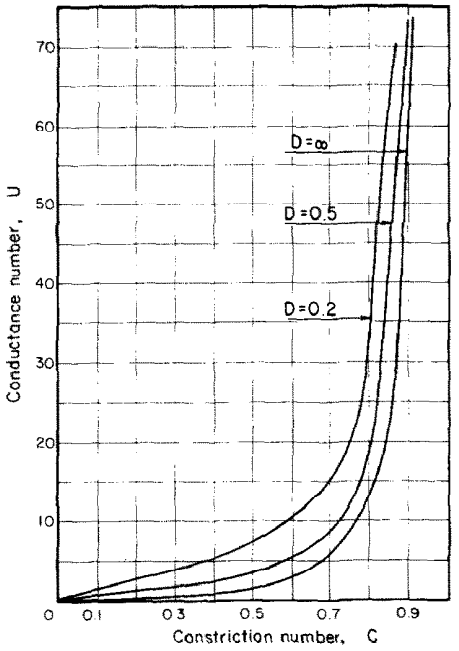

FIG. 3. Constriction number C vs U for $K = 0$ (planar contact).

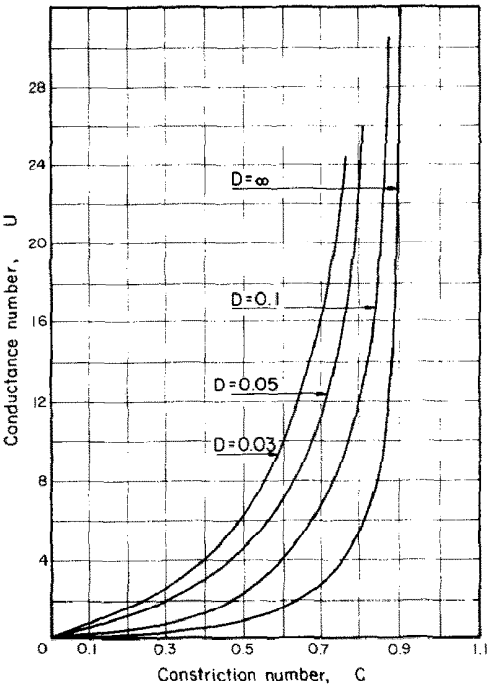

FIG. 4. Constriction number C vs U for $K = 0$ (circular contact).

If R_T is the total resistance with constriction, then

$$R_T = \frac{\Delta T}{Q} = \frac{T_1 - 0}{Q} \tag{22}$$

and if R_0 is the total resistance with no constriction, then

$$R_0 = \frac{l}{K_1(\pi a)^p a} = \frac{D}{K_1(\pi a)^p}. \tag{23}$$

The resistance due to constriction for solid 1 is given by

$$R_{c_1} = R_T - R_0. \tag{24}$$

The total conductance u_{c_1} is given by

$$u_{c_1} = \frac{1}{R_{c_1}}. \tag{25}$$

Since the conductance components of solid 1 and 2 are in series, then

$$\frac{1}{u_c} = \frac{1}{u_{c_1}} + \frac{1}{u_{c_2}}. \tag{26}$$

Substituting equations (21)–(24) in (26) and rearranging, we get

$$u_c = \frac{(\pi a)^p K_s}{2\left[\dfrac{1}{2^p\left[-\dfrac{G_0}{p+1} + \displaystyle\sum_{n=1}^{\infty} G_n \int z^p \phi(\lambda_n z)\,\mathrm{d}z\right]} - D\right]}. \tag{27}$$

The contact conductance per unit area u is then given by

$$u = \frac{u_c}{(\pi a)^p a}. \tag{28}$$

Combining equation (27) and (28), the dimensionless contact conductance is given by

$$U = \frac{ua}{K_s} = \frac{1}{2\left[\dfrac{1}{2^p\left[-\dfrac{G_0}{p+1} + \sum_{n=1}^{\infty} G_n \int_0^1 Z^p \phi(\lambda_n Z)\,dZ\right]} - D\right]}. \tag{29}$$

The dimensionless contact conductance for a planar, as well as circular contact from equation (29), can be derived to be

$$U = -\frac{G_0}{2(1+DG_0)}. \tag{30}$$

3.4. *Comparison of present solution with existing theories*

The general solution for thermal contact conductance of planar and circular contacts with interstitial fluids are in the form of infinite series. To obtain exact numerical results, all of the terms must be evaluated. This is not possible in practice. It then becomes important to know the number of terms of the series to be used for reasonable accuracy. A closed form exact solution for planar contacts exists in vacuum (i.e. $K = 0$), with which present theory can be compared. This special case closed form solution can be written as [13]

$$U_{c0} = \frac{\pi}{4\ln\left[\dfrac{1}{\sin\left(\dfrac{\pi c}{2}\right)}\right]}. \tag{31}$$

Where U_{c0} is the dimensionless contact conductance of the closed form solution. The percentage deviation of the series solution, defined as $100(U - U_{c0})/U_{c0}$, has been calculated for several cases by varying the constriction number C and the factor ξ. The damping factor ξ and the number of terms are related in [14] as

$$\xi = 8N - 7. \tag{32}$$

Using ξ given by this formula, the percentage deviation has been calculated for nine different C's and four different N's. The results are presented in Table 1. The value of D for this table is 2.

Table 1. Comparison of closed form and series solutions for conductance of planar contacts in vacuum

		Percentage deviation $100(U_0 - U_{c0})/U_{c0}$		
C	U_{c0}	$N = 10$	$N = 20$	$N = 30$
0.1	0.423	13	7	1
0.2	0.669	10	5.0	1.5
0.3	0.995	8.8	5.0	2
0.4	1.478	5.0	2.0	1.2
0.5	2.266	1.1	1.0	1.0
0.6	3.706	0.8	0.45	0.32
0.7	6.805	0.6	0.35	0.27
0.8	15.651	0.35	0.2	0.15
0.9	63.502	0.2	0.1	0.09

We could not go beyond $N = 30$ because of the term $(N\pi D)$ and its hyperbolic sine and cosine functions. As seen from the table, the percentage deviation is very nominal and it can further be reduced by taking more terms in the infinite series.

For comparison of solutions for the thermal contact conductances of circular contacts having interstitial fluids, the theories given in [10] have been rewritten in terms of dimensionless numbers used and the percentage deviation of each earlier theory (U) from the present theory (U_0) defined by $100(U - U_0)/U_0$, has been calculated for several combinations of constriction numbers (C) and the ratio K/B. The value of (D) has been kept at 2. The relationship between ξ and the number of terms is given by equation (32). The comparison is shown in Table 2.

Table 2. Comparison of present theory and solutions for contact conductance of semi-infinite cylindrical contact elements

		Percentage deviation from present solution $= 100(U - U_0)/U_0$	
C	K/B	U_0	[10]
0.1	10^{-4}	0.15	−19.26
	10^{-2}	0.16	−17.18
	1	1.30	4.38
	10^2	114.51	−11.59
0.3	10^{-4}	0.45	−12.4
	10^{-2}	0.488	−14.33
	1	2.20	−19.24
	10^2	114.81	+23.23
0.5	10^{-4}	1.42	−33.9
	10^{-2}	1.44	−33.95
	1	2.92	−20.2
	10^2	138.3	−2.28
0.7	10^{-4}	3.79	−16.1
	10^{-2}	3.81	−16.01
	1	5.97	−11.89
	10^2	205.38	−1.933
0.9	10^{-4}	33.34	−5.24
	10^{-2}	33.40	−5.26
	1	39.2	−4.97
	10^2	587.95	−3.00

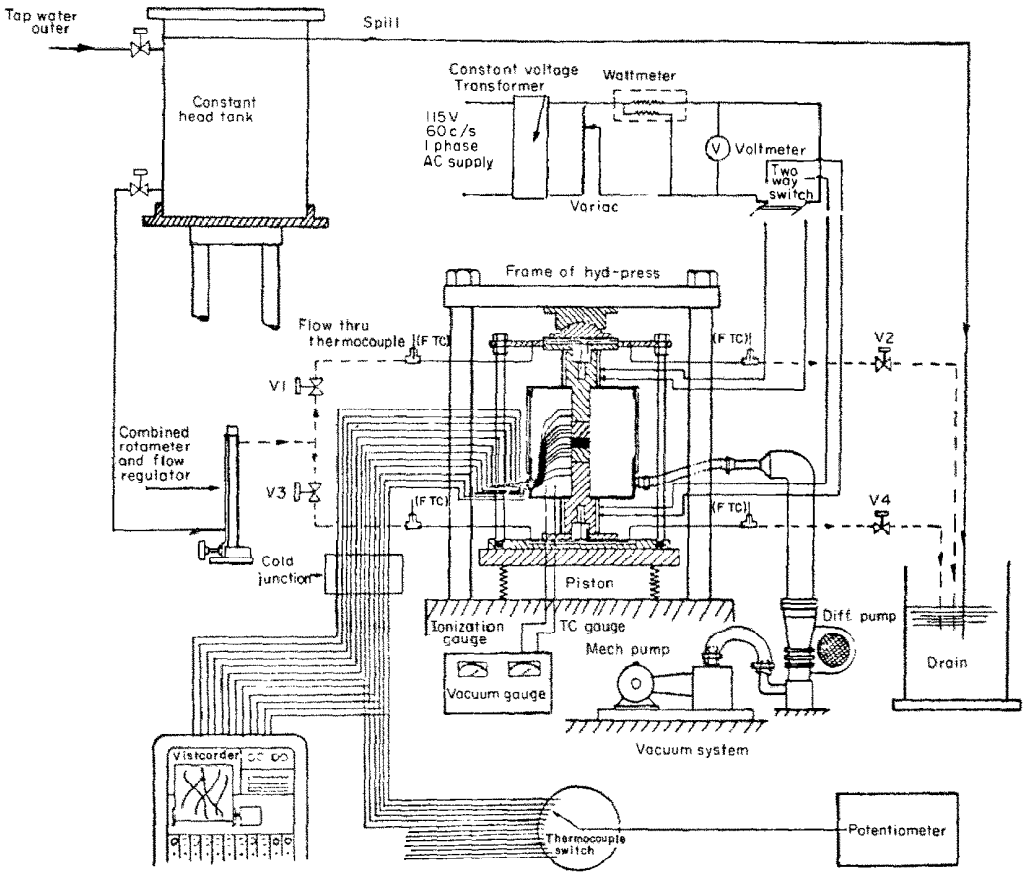

FIG. 5. Schematic diagram of test set-up.

A study of Table 2 shows that the theory of [10] has significant deviation from the present solution. One point has to be noted here: The results are for semi-infinite cylindrical contact elements and our assumption of $D = 2$, obviously, brings some error.

4. TEST APPARATUS AND PROCEDURE

4.1. *General description*

Figure 5 presents a schematic of the experimental set-up. The test chamber is shown in Fig. 6. The test piece assembly with upper and lower heat flow meters is given in Fig. 7. The test assembly was composed of 51 laminated metal disk test pieces and different interstitial fluids. The test assembly was equipped with 3 thermocouples, at equal intervals, to measure the axial temperature profile in it. The test assembly was located between two heat flow meters. The heat flow meters were each equipped with four thermocouples to measure the heat flow rate passing through before and after the test assembly. The heat flow meters were held in a vertical position by heater–cooler units originating from top and bottom flanges. Continuation of the heater–cooler units on the outside of the upper and lower flanges form built-in type heat sinks with running water, and band heaters as heat sources. The test assembly, the heat flow meters, and the heater–cooler units formed a vertical cylindrical column which was loaded axially by a hydraulic press.

4.2. *Test assembly*

Test pieces were made of laminated metal disks of 2.54 cm (1.00 in) dia and thickness typically 0.0025 cm (0.010 in). Different interstitial fluids were used to fill the voids between the mating test piece surfaces. Each test assembly was performed with fifty-one test pieces. Three thermocouples were located, spaced equally, in each test assembly. The following description gives the test piece preparation.

(a) *Test pieces.* Test pieces were made from magnetic core steel, yellow brass, aluminum (7075-T6) and stainless steel 302. Their properties are given in Table 3. The following procedures were used in preparation of the test pieces.

(b) *Fabrication.* The first process was flattening the metal sheet as precisely as possible. Circular disks were cut from the metal sheet by stamping and the outside edges were removed by filing. The test pieces were then covered with oil. This prevented oxidation and scratching.

(c) *Cleaning.* The metal disks were first dipped into Xylene (a very strong dissolver) and rinsed with acetone, then dried with a paper towel.

(d) *Heat flow meters.* Heat flow meters were made from Monel K-500. The contact surfaces were machined flat and then polished near to optical flatness. Then holes were drilled on their surfaces to fix thermocouple leads.

(e) *Heater–cooler units.* Special nickel chromium

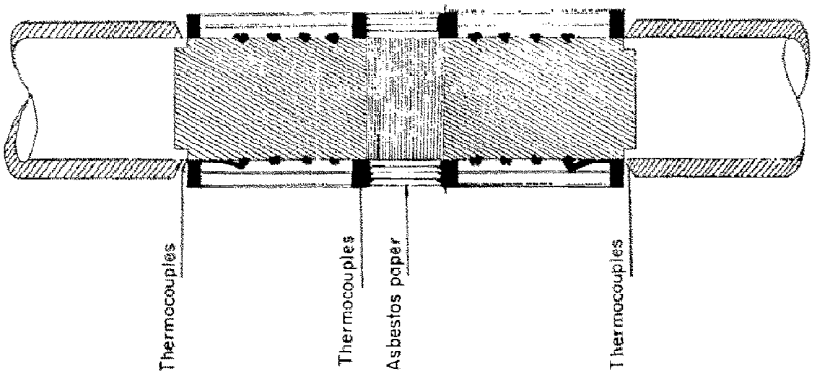

Fig. 7. Detail of assembled test specimen and heat flow meters.

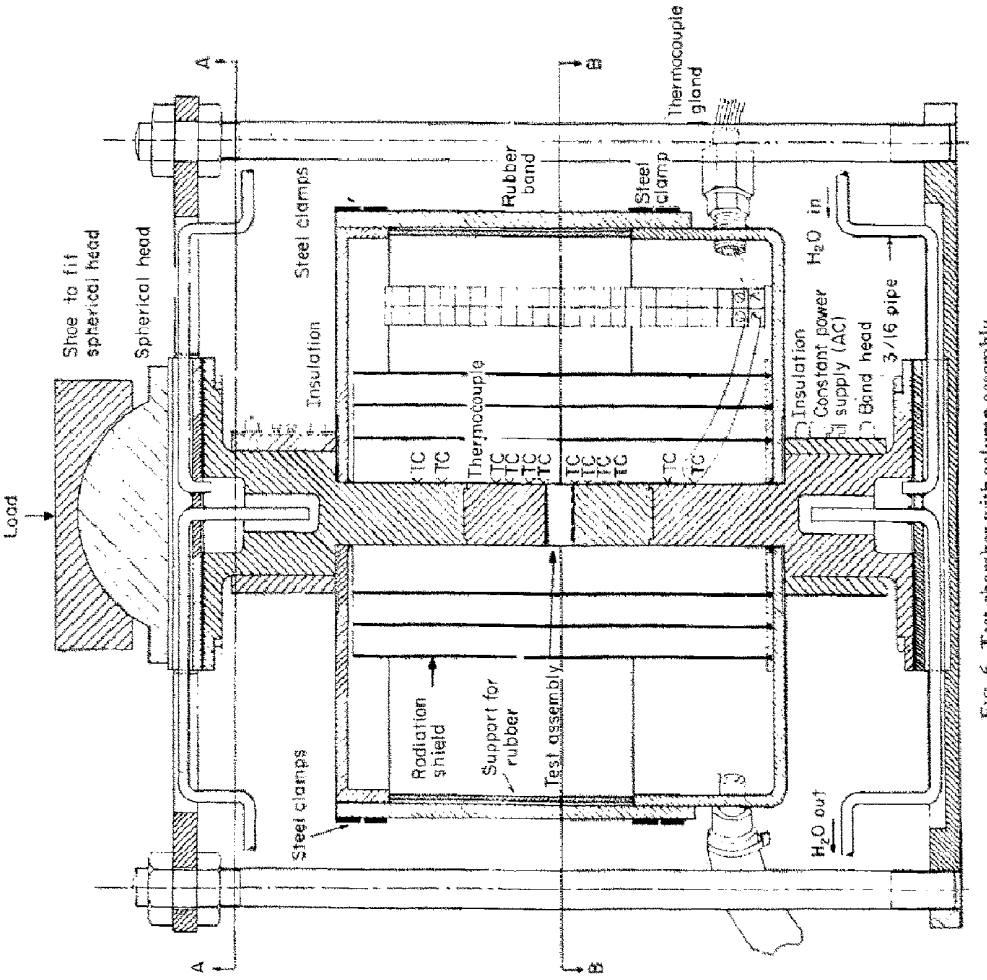

Fig. 6. Test chamber with column assembly.

Table 3. Dimension of the test piece and test assembly

Test piece material	Diameter (in)	Test piece thickness (in)			Test assembly: Thermocouple distance from upper contact (in)			Surface roughness (in)			Number of test pieces in test assembly
		Metal	Coating	Total	Y_1	Y_2	Y_3	Before test	After test	Decrease %	
Magnetic core I	0.9930	0.013	2 × 0.0005	0.014	0.175	0.357	0.539	62.00	56.5	8.9	51
Magnetic core G.E.	1.0650	0.0133	2 × 0.00025	0.0138	0.1725	0.3519	0.5313	33.23	29.62	10.8	51
Yellow brass	0.9930	0.01		0.01	0.125	0.255	0.385	11.08	10.7	3.5	51
Aluminum 7075 T6	0.9930	0.01		0.01	0.125	0.225	0.385	12.913	12.1	6.3	51
Stainless steel 302	0.9930	0.01		0.01	0.125	0.225	0.385	26.96	26.23	2.7	51

alloy (Inconel alloy 600) was used for the upper and lower flow meter holders in order to withstand high pressures and temperature.

(f) *Radiation shields.* Two semi-cylindrical radiation shields, each made by three concentric cylindrical sheets of aluminum, were mounted by means of screws to an aluminum base. The distance between the radiation shield sheets was 1.2 cm. Inner surface of the shields was aluminum, and the outer surfaces were painted black.

(g) *Loading system.* The loading system consisted of a hydraulic press with a capacity of 60 tons. The load was applied by turning the hand wheel through the use of a lever bar. Pressure through the aluminum adaptor (a circular asbestos disk and flange of the upper heater–cooler unit) was transmitted to the test assembly.

5. RESULTS

Figures 8–11 show the measured and predicted values of conductance of stacks of laminations and indicate good agreement.

Figure 8 reports the experimental data of Williams [4] whose steel sheets were coated with an insulating enamel. The theoretical conductance, based on bare steel sheets, is consistently higher than the measured value as would be expected due to neglecting the effect of the thin enamel layers. It is believed that the agreement would be improved by about 15% if the effect of the enamel were included, but there is insufficient information to confirm this.

For steel sheets in a vacuum environment, the correlation between this theory and the measurements of Thomas and Probert [2] is given in Fig. 9. Apart from the region of lowest contact pressure, the

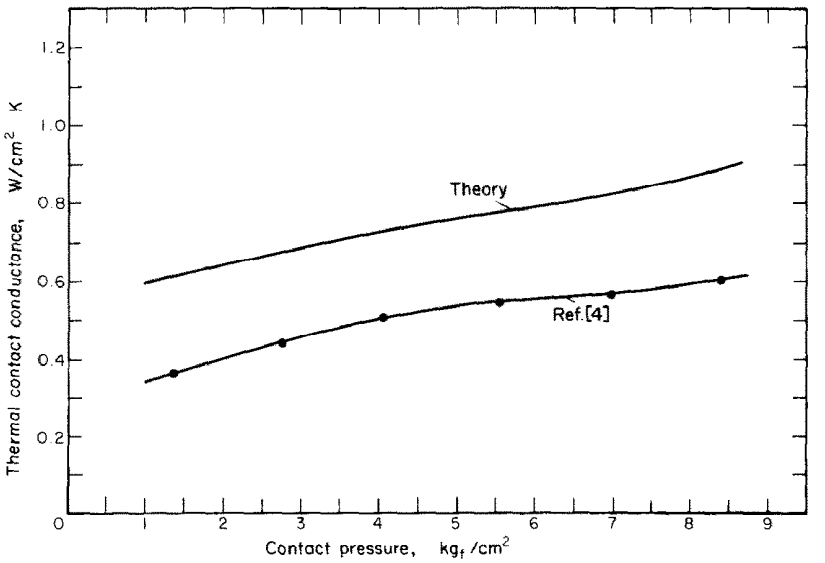

FIG. 8. Steel elements in environment of air.

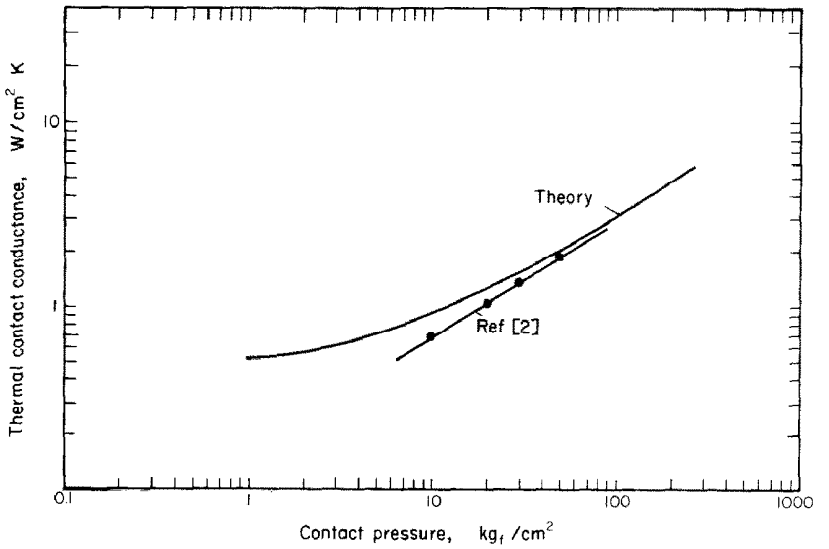

FIG. 9. Steel elements in vacuum.

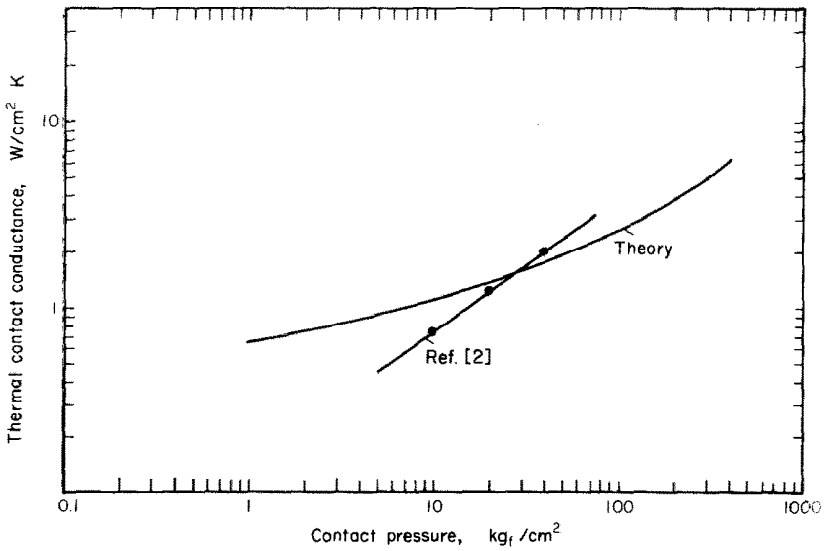

FIG. 10. Brass elements in vacuum.

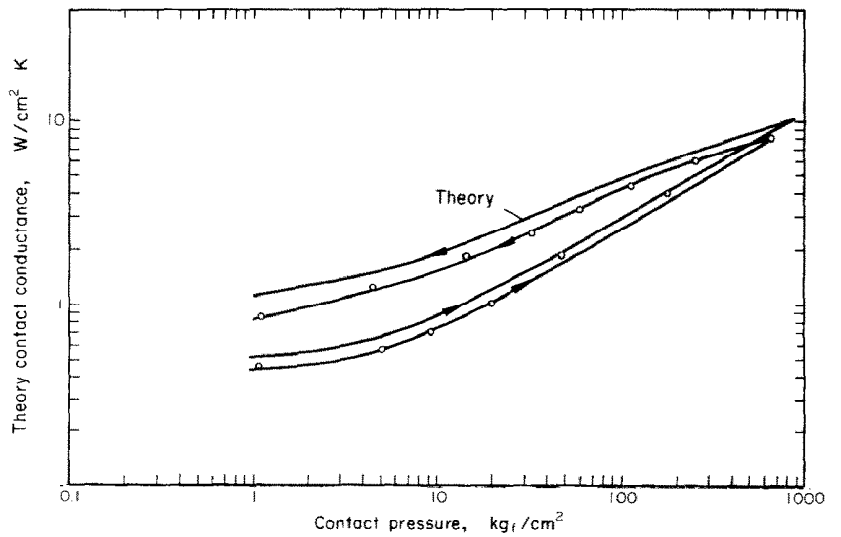

FIG. 11. Stainless steel elements in air showing hysteresis in conductance during unloading.

correlation is excellent. Brass contacts are not so well predicted, see Fig. 10; the two curves appear to indicate that an incorrect value of hardness had been used in the prediction. At this stage, it is not possible to recheck the hardness values of the test specimens.

Figure 11 shows the hysteresis effect on conductance when the contact pressure is first increased, then decreased. With stacks of thin laminations, any deviations from flatness of the sheets will cause the stack to act as a spring. To estimate the conductance during the decreasing pressure segment, it is necessary to separate the components of contact area due either to elastic or to plastic deformation. Figure 11 shows that this separation is now predictable, as the theoretical behavior of stainless steel sheets matched closely their test measurements.

It should be noted that the good agreement extends over the wide range of contact pressure from 1.5×10^5 N/m^2 to 650×10^5 N/m^2. In any specific application of a laminated component for which the contact pressure would probably be controlled within a small range, the prediction may be further refined by concentrating on the parameters appropriate to that pressure band. The theory appears to have valuable application in the design of electrical transformers and machinery.

6. CONCLUSIONS

A theory has been developed for the steady state thermal conductance of stacks of metallic sheets. It predicts the effect on conductance of varying the contact pressure over a range of pressure from 1.5 N/m^2 to 650×10^5 N/m^2, and for both increasing and decreasing loadings. Good agreement between predictions and test measurements are seen for stacks of stainless steel, brass, and transformer core steel for several different interstitial fluids. The theory is believed to be of direct use to the designers of electrical transformers, motors, generators, and similar equipment.

Acknowledgement—The authors wish to express their appreciation to Dr. H. Yüncü for his interest, valuable suggestions and assistance.

REFERENCES

1. R. P. Mikesell and R. D. Scott, Heat conduction through insulating supports in very low temperature equipment, *J. Res. Nat. Bur. Stand.* **57**, 371–376 (1956).
2. T. R. Thomas and S. D. Probert, Thermal resistances of some multi-layer contacts under static loads, *Int. J. Heat Mass Transfer* **9**, 739–754 (1966).
3. T. J. Roberts, Determination of the thermal constants of the heat flow equations of electrical machines, *Proc. Instn Mech. Engrs* **184**(3E), 84–90 (1969–70).
4. A. Williams, Heat flow through stacks of steel laminations, *J. Mech. Engng Sci.* **13**, 217–223 (1971).
5. A. Williams, Experiments on the flow of heat across stacks of steel laminations, *J. Mech. Engng Sci.* **14**, 151–154 (1972).
6. B. B. Mikic and G. Cornasciali, The effect of thermal conductivity of plating material on thermal contact resistance, *J. Heat Transfer* **92**, 475–482 (1970).
7. J. Molgaard and W. W. Smeltzer, Thermal contact resistance at gold foil surfaces, *Int. J. Heat Mass Transfer* **15**, 1151–1162 (1970).
8. L. S. Fletcher, Thermal contact resistance of metallic interfaces, AIAA Paper No. 70-852, 8 (1970).
9. L. S. Fletcher and R. G. Miller, Thermal conductance of gasket materials for space craft joints, AIAA Paper No. 73-119, 9 (1972).
10. T. N. Veziroğlu, H. Yüncü and S. Kakaç, Analysis of thermal conductance of contacts with interstitial plates, *Int. J. Heat Mass Transfer* **19**, 959–965 (1976).
11. E. R. Gale, Effects of surface films on thermal contact conductance, Part I—Microscopic experiments, ASME Paper 70 HT/SpT-27, 8 (1971).
12. Y. H. Tsao and R. W. Heimburg, Effects of surface films on thermal conductance, Part 2—Macroscopic experiments, ASME Paper 70 HT/SpT-27, 7 (1971).
13. P. Nayak, Thermal contact conductance of stacks, Ph.D. Dissertation, University of Miami, Mechanical Engineering Dept., (1977).
14. T. N. Veziroğlu, M. A. Huerta and S. Kakaç, Exact solutions for thermal conductances of planar and circular contacts, Presented at the *14th International Conference on Thermal Conductivity*, University of Connecticut (June 1975).

CALCUL ET MESURE DE LA CONDUCTANCE THERMIQUE DES EMPILEMENTS LAMELLAIRES

Résumé—On présente une nouvelle analyse théorique de la conductance thermique de contact entre les feuilles métalliques minces. Les théories antérieures s'appliquent uniquement au cas où l'épaisseur de métal est grande en comparaison du diamètre caractéristique de la zone de contact. La nouvelle théorie présentée ici calcule les empilements de lamelles pour une large gamme de pression de contact et avec des fluides interstitiels variés. On a expérimenté sur des disques métalliques d'acier inoxydable, de cuivre et d'acier pour coeur de transformateur, et les conductances mesurées sont comparées au valeurs calculées. L'accord entre théorie et expérience est bon, à la fois pour les mesures faites dans cette étude et pour les données expérimentales déjà publiées.

BERECHNUNG UND MESSUNG DER THERMISCHEN LEITFÄHIGKEIT GESCHICHTETER KÖRPER

Zusammenfassung—Die Arbeit beschreibt eine neue analytische Methode zur Berechnung des thermischen Kontaktwiderstandes zwischen dünnen Metall-Folien. Ältere Theorien lassen sich nur auf Fälle anwenden, bei denen die Dicke der Metallschicht groß ist im Vergleich zum Durchmesser einer typischen Kontaktzone. Die neu entwickelte Theorie wird auf die Berechnung der Leitfähigkeit von vielfach geschichteten Körpern in einem weiten Bereich von Kontaktdrücken und für verschiedene Kontaktflüssigkeiten angewendet. Folien aus rostfreiem Stahl, Messing und Transformatorenblech wurden untersucht und die gemessene Leitfähigkeit mit den Ergebnissen der Rechnung verglichen. Die Übereinstimmung zwischen Theorie und Experiment war gut sowohl bei den eigenen Versuchen als auch für die erreichbaren veröffentlichten experimentellen Werte.

РАСЧЁТ И ИЗМЕРЕНИЕ ТЕПЛОПРОВОДНОСТИ ТЕЛ, СОСТОЯЩИХ ИЗ НАБОРА ПЛАСТИН

Аннотация — В статье представлен новый теоретический анализ контактной теплопроводности между тонкими металлическими пластинами. Существующие методы применимы только к случаю, когда толщина металлической пластины велика по сравнению с характерным размером контактной зоны. Предложенный метод использовался для расчета теплопроводности наборов пластин с различными жидкостями в широком диапазоне изменения контактного давления. Экспериментально исследовались диски из нержавеющей стали, латуни и стали для трансформаторных сердечников. Сравнение экспериментальных данных с расчетными обнаружило хорошее соответствие как с результатами экспериментов настоящей работы, так и данными других авторов.